Modulated Phases Observed in Reacting Polymer Mixtures with Competing Interactions

Asuka Harada† and Qui Tran-Cong*

Department of Polymer Science and Engineering, Kyoto Institute of Technology, Matsugasaki, Sakyo-ku, Kyoto 606, Japan

Received October 21, 1996; Revised Manuscript Received January 2, 1997[⊗]

ABSTRACT: Reaction-induced phase separation of polymer blends was examined by optical microscopy in this work. Four distinct types of ordering processes were observed when a miscible polymer blend was photo-cross-linked in the one-phase region located between the coexistence curve and the glass transition temperatures. These structures, known as modulated phases, emerge from the competitions between phase separation, which acts as a short-range activation process, and the cross-linking reaction, contributing as a long-range inhibition effect. Because of the network formation, elasticity participates as an additional long-range interaction at the late stage of the reactions, making the problem more interesting and complex. These structures and their ordering kinetics observed under various experimental conditions were analyzed and classified by the morphological phase diagram constructed from the experimental data. These results are discussed in terms of pattern selection driven by the competitions between photo-cross-linking reactions and phase separation of polymer blends.

I. Introduction

Phase separation associated with chemical reactions is a fascinating phenomenon which is not only related to basic problems of physics such as modes selection in systems far from equilibrium[1] but also directly connected to various practical aspects of polymer materials such as reactive processing[2] and photoresist and/or photoimaging of materials containing multicomponent polymers.[3] Among various types of chemical reactions, cross-linking is widely used in these processes. For most cases, miscible polymer blends are destabilized by cross-linking reactions and undergo phase separation. These phenomena are often observed during the preparation of interpenetrating polymer networks (IPN)[4] where the morphology resulting from phase separation plays a crucial role in modifying the physical properties of these polymer materials.

In general, the morphology induced by cross-linking reactions is controlled by the rates of the reaction and the phase separation. The former tends to suppress the phase separation by slowing down the polymer chain diffusion, whereas the latter is activated by the reaction via thermodynamical instabilities. In other words, the behavior of the reacting blend is controlled by two antagonistic effects: cross-linking reaction and phase separation. The former is relatively a long-range effect compared to the latter because the reaction amplifies the concentration fluctuations which, in turn, accelerate the reaction and thermodynamically destabilizes the blends. It has been known that systems in which there exist the competitions between antagonistic interactions taking place at different length scales can exhibit a wide range of periodic structures called modulated phases. These spatially ordering phenomena have been found in a variety of physical as well as chemical systems ranging from ferrofluids under a magnetic field to Langmuir monolayers at an air−water interface.[5] Depending upon the strengths of these antagonistic interactions, the characteristic length scales of these modulated phases can vary from nanometer (e.g. in the ripple phase of vesicles[6]) to centimeters (e.g. in Rayleigh−Bénard instabilities of gas and/or liquids[7]). In polymer materials, block copolymers are known to exhibit modulated phases due to the competitions between the short-range attraction and the long-range repulsion of immiscible components which are forced to be linked together on a chain by chemical bondings. Since the molecular weights of these block copolymers are limited by the current synthesis techniques, the sizes of these ordered phases are restricted in the nanometer scale.

In this paper, we experimentally show that binary polymer blends with one component undergoing photo-cross-linking can become unstable and exhibit a wide range of stable structures, i.e. the so-called modulated phases, which differ from those observed for the spinodal decomposition process in the absence of chemical reactions. At first, the experimental procedures are described in detail. Subsequently, the ordering kinetics of these modulated phases obtained under various conditions are analyzed and classified by the morphological phase diagram constructed from these data. Finally, the mechanisms of these ordering processes and the perspective of morphological architecturing for multiphase polymeric materials based on reacting polymer blends are discussed in terms of pattern selection processes driven by chemical reactions.

II. Experimental Section

(A) Samples. Polymer blends used in this work are the mixtures of poly(styrene-*stat*-(chloromethyl)styrene) (PSCS) and poly(vinyl methyl ether) (PVME). The former was prepared by copolymerization of styrene (Wako Chemicals, Japan) and (chloromethyl)styrene (Tokyo Kasei, Japan) according to the procedure described previously.[8] The content of (chloromethyl)styrene in the copolymer is 13.9 mol %, as estimated from the elemental analysis. The molecular weight of PSCS and its distribution are $M_w = 2.6 \times 10^5$ and $M_w/M_n = 1.5$, respectively. Poly(vinyl methyl ether) (PVME, Aldrich, $M_w = 9.6 \times 10^4$, $M_w/M_n = 1.8$) was reprecipitated using toluene as a good solvent and *n*-heptane as a nonsolvent. In order to perform the photo-cross-linking reaction, anthracene as a cross-linker was labeled on the chloromethyl moieties of PSCS chains, as reported previously.[8] The label content of the PSCS chains is ca. 1 anthracene per 40 repeating units of the polymer. All the samples were obtained by casting toluene solutions containing appropriate amounts of PSCS and PVME.

* To whom correspondence should be addressed.
† Currently with DaiNippon Ink & Chemicals Inc., Sakai, Japan.
⊗ Abstract published in *Advance ACS Abstracts*, February 15, 1997.

S0024-9297(96)01542-2 CCC: $14.00 © 1997 American Chemical Society

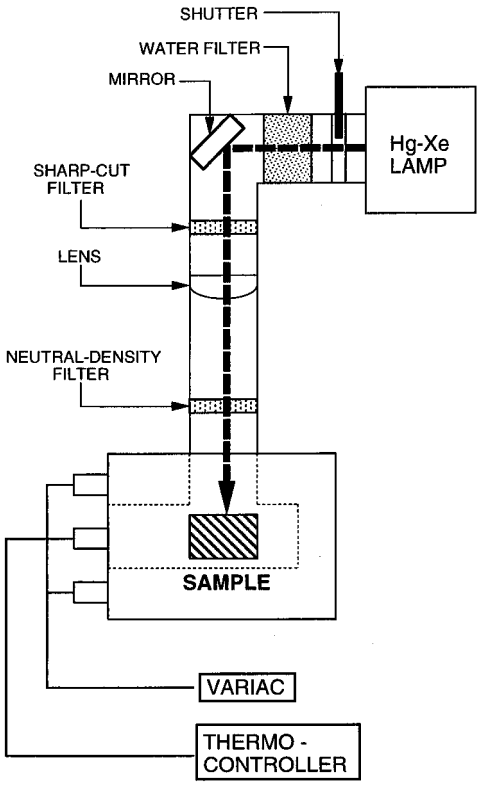

Figure 1. Setup for the irradiation experiments performed in this work.

The mixture with a given composition was mounted into an aluminum spacer (6 mm x 12 mm × 50 μm) and dried in vacuo at 90 °C over 2 nights. Finally, the sample was sandwiched between two pieces of slide glass prior to the experiments.

(B) Irradiation Experiments. The setup for the irradiation experiments is shown in Figure 1. Ultraviolet (UV) light from a mercury−xenon (Hg−Xe) lamp (500 W, Hamamatsu Photonics) was first passed through a water filter of 5 cm path length to remove the infrared components from the light source. Subsequently, the UV components were allowed to reflect at a flat mirror coated with dielectric multilayers (Sigma Koki, Japan). A sharp-cut filter (SC-052, Corning) was used to completely eliminate the light with wavelengths shorter than 300 nm. The incident light obtained in this way was then focused at the sample placed horizontally in a brass heating block thermostated with the precision ±0.5 °C. Finally, the intensity of irradiation was adjusted by using a neutral density filter positioned in the front of the sample. Throughout this work, the UV light intensity at 365 nm was fixed at 3.0 mJ/(cm^2·s). Furthermore, to release the elastic stress accumulated during the reaction toward the un-cross-linked peripheral of the sample, only the middle part (4 mm × 8 mm) of the blend (6 mm × 12 mm × 0.05 mm) was irradiated using a black metallic mask. It is worth noting that for the masks with diameters larger than 2 mm, the morphology of the irradiated blends was not affected by the mask sizes. In this work, the photo-cross-linking reaction was performed with the three compositions PSCS/ PVME (20/80), (50/50), and (70/30) in the one-phase region of the blend.

(C) Instruments. (1) Cloud Points and Glass Transition Temperatures. The cloud points of PSCS/PVME blends were obtained by light scattering at a fixed angle (20°) under four different heating rates 0.1, 0.2, 0.5, and 1 °C/min. The temperature corresponding, in principle, to the phase equilibrium was obtained by extrapolating these data to zero-heating rate. As reported previously, PSCS/PVME blends possess a lower critical solution temperature (LCST).[8] On the other hand, the glass transition temperatures (T_g) of these blends were measured by using differential scanning calorimetry (Mac Science, DSC-3100) with a heating rate of 5 °C/min. The T_g of a blend with a given composition was determined from the midpoint transition of the thermogram.

(2) Phase Morphology. The morphology of these cross-linked blends was observed by using a phase-contrast optical microscope (Nikon, Model XF-NTF-21). The focus was set at the middle of the reacting blends, and the emerging morphology was observed at the same position of the blends after irradiation over different time intervals. The optical images of the phase-separated structures were transferred to a digital image analyzer (Pias, LA-525) where the 2-dimensional fast Fourier transfom (2D-FFT) was performed for structural analysis. From the power spectra, the characteristic length scales ξ of the structures were calculated by using the Bragg condition $\xi = 2\pi/q_{max}$ where q_{max} is the frequency corresponding to the maximum magnitude of the 2D-FFT power spectra.[9] The threshold where the sample becomes cloudy during irradiation is determined by monitoring the absorbance of the blend at 500 nm located outside of the absorption range of anthracene.

III. Results and Discussion

PSCS/PVME blends were irradiated in the one-phase region limited by the coexistence curve and the glass transition temperatures. In general, when the PSCS component is cross-linked, the blends become unstable and the coexistence curve shifts toward the lower temperature side. Phase separation begins as soon as the new coexistence curve crosses the experimental temperatures. There are two extreme cases for the experiments: one is cross-linking the blend in the vicinity of the coexistence curve, and the other is close to the glass transition temperatures of the blend. The former corresponds to the case of deep quench because the phase boundary of the blends crosses the experimental temperatures at low cross-linking densities. On the other hand, the latter case corresponds to the shallow quench conditions and only metastably miscible semi-IPNs or microphase separation are observed because the phase boundary of the blends reaches the experimental temperatures at very high cross-linking densities. In the intermediate range between these two limits, a variety of ordered structures emerges depending upon the balance between the reaction and the phase separation.

(1) Phase Separation Induced by a Photo-Cross-Linking Reaction in the Vicinity of the Phase Boundary. In order to examine the effects of cross-linking reactions in the vicinity of the coexistence curve, PSCS/PVME blends with the three compositions (20/80), (50/50), and (70/30) were irradiated at temperatures located within 20 °C of their corresponding cloud points. For all these three compositions, PSCS/PVME blends undergo phase separation, exhibiting the typical interconnecting structures of the spinodal decomposition process. As an example, the morphology observed for a PSCS/PVME (20/80) blend photo-cross-linked over 55 min at 110 °C is shown in Figure 2a. The corresponding power spectra obtained by 2D-FFT are illustrated in Figure 2b. It was found that after 10 min of cross-linking, the phase boundary of this reacted blend has already crossed the experimental temperatures (110 °C). From the irradiation time dependence of the 2D-FFT power spectra, the characteristic length scale (ξ) of these interconnecting structures was calculated by using the Bragg condition as described in section II. It was found that ξ grows in a short period of time and eventually approaches an equilibrium value of ca. 2 μm after 30 min of irradiation, as illustrated in Figure 3. Here, the characteristic length ξ was plotted versus irradiation time in the double logarithmic scale. It can be seen that before being frozen, the growth of these structures with the cross-linking time t can be well expressed by the

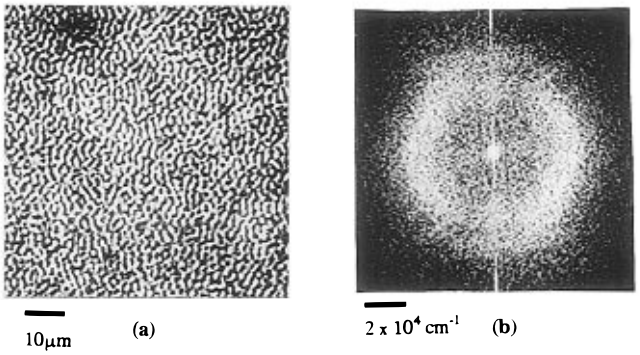

Figure 2. (a) Phase-contrast optical micrographs of a PSCS/PVME (20/80) blend irradiated at 110 °C over 55 min. (b) Corresponding 2D-FFT power spectra.

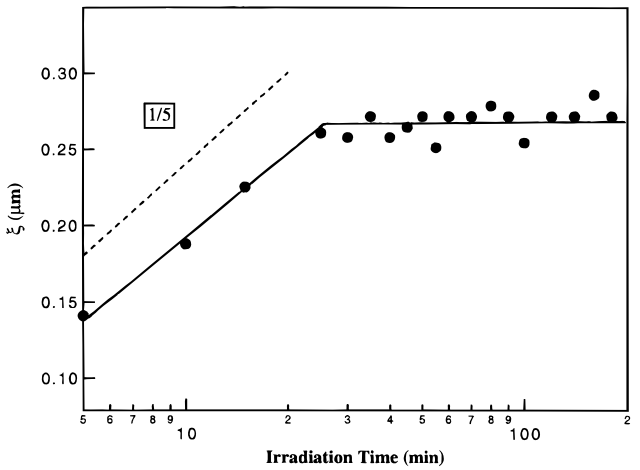

Figure 3. Time evolution of the characteristic length scale ξ of the interconnecting structures observed for a PSCS/PVME (20/80) blend cross-linked at 110 °C.

power law $\xi \propto t^{\alpha}$ where α is approximately 1/5 for this particular composition. Similar behavior was also observed for PSCS/PVME (50/50) and (70/30) blends photo-cross-linked in the region close to the coexistence curve. The exponents α found for these two compositions at 120 and 130 °C are approximately 1/4 and 1/3, respectively. In an early communication,[10] it has been reported that the phase separation kinetics observed under these conditions follows the scaling law proposed for the phase separation in the presence of obstacles.[11] These exponents reflect the behavior of phase separation arising from different cross-linking kinetics due to the change in anthracene concentrations with the blend composition. The details of these kinetics are reported elsewhere.[12] Because the sample is continuously irradiated, the forming PSCS networks tend to suppress these processes. The extent to which the phase separation can proceed depends upon the cross-linking kinetics and also on the cloudiness generated by the coalescence of phase-separated domains in the blend. Particularly, the latter prevents the photochemical reaction from proceeding further under irradiation. Because the viscosity of the blend increases with the network fraction in the blend, phase separation is gradually slowed down and eventually frozen during irradiation. As mentioned earlier, the above results were obtained under deep quench conditions and are strongly in contrast with the cases observed at lower temperatures corresponding to the shallow quench conditions.

Another extreme case is carrying out the reaction in the vicinity of the glass transition temperature (T_g) of the blends. Since the experimental temperatures are far away from the phase boundary, the cross-linking density as well as the T_g of the blends becomes very high before the blends start phase separating. The sample obtained under these conditions is a thermodynamically frustrated system because PVME chains are kinetically trapped by the PSCS networks and cannot diffuse to facilitate the phase separation. Therefore, annealing the blends at high temperatures after cross-linking leads to the formation of microdomains in the nanometer range.[8]

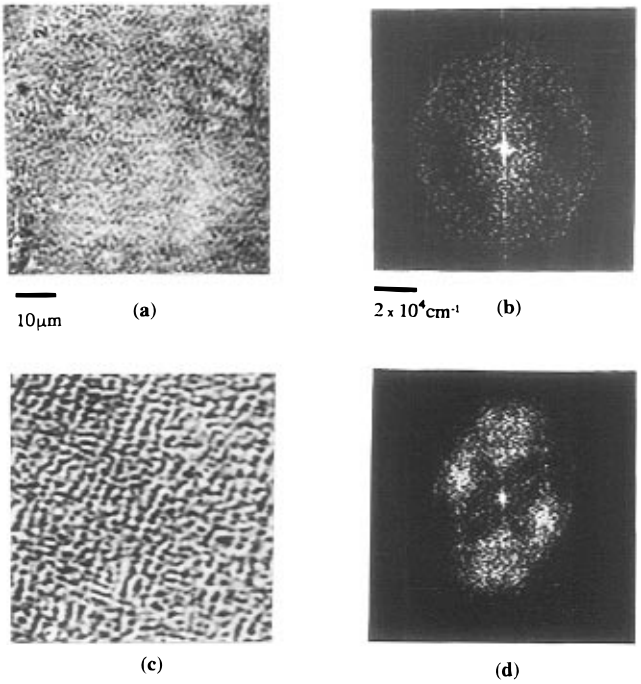

Figure 4. Phase-contrast optical micrographs of a PSCS/PVME (20/80) blend irradiated at 80 °C over (a) 1 h and (c) 5 h. (b) and (d) are the 2D-FFT power spectra corresponding respectively to (a) and (c).

(2) Photo-Cross-Linking Reactions Performed in the Intermediate Range of Temperatures. Phase separation initiated by irradiation at temperatures located between the cloud points and T_g of the unreacted blends is particularly interesting because the effects of phase separation become comparable to those of the cross-linking reactions. Depending upon the strengths of these competition processes, the following ordered structures have been found in this range of temperatures.

(a) Labyrinthine Structures. These structures were observed for PSCS/PVME (20/80) blends photo-cross-linked between 80 and 100 °C. Phase separation of the blend becomes observable by phase-contrast optical microscopy at 45 min after irradiation. At the early stage, these structures are isotropic, as revealed by 2D-FFT power spectra as shown in Figure 4a,b for a PSCS/PVME (20/80) blend photo-cross-linked at 80 °C over 60 min. As the irradiation time increases, their contrast and then their length scales increase. The morphology is isotropic and cocontinuous within 90 min of irradiation. During this period of time, the length scales of the structures are almost unchanged with irradiation time while the contrast increases. These results suggest that the phase separation process induced by the cross-linking reaction probably passes through the linear region predicted by the Cahn–Hilliard theory.[13] However, after 90 min, these structures become larger and gradually turn to anisotropic labyrinth-like patterns, as illustrated in Figure 4c and

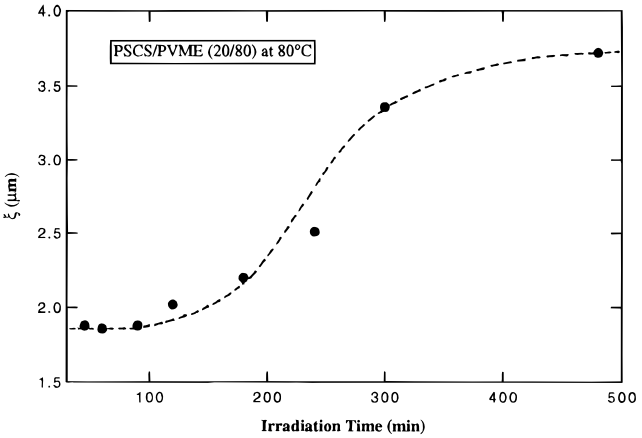

Figure 5. Time evolution of the characteristic length scale of the labyrinthine structures obtained for a PSCS/PVME (20/80) blend photo-cross-linked at 80 °C.

verified by the 2D-FFT power spectra in Figure 4d. For longer irradiation times, the ordering process proceeds further, resulting in highly regular structures, as revealed by the second order of diffraction patterns reported previously.[14] Eventually, these structures are frozen by the high cross-linking density. Similar behavior was observed with PSCS/PVME (20/80) cross-linked at 90 and 100 °C. The dependence of the characteristic length scales ξ of these structures on irradiation time was examined at a particular direction of the 2D-FFT power spectra. As an example, ξ at 160° with respect to the *X*-axis of the power spectra obtained at various irradiation times was calculated from the Bragg condition and shown in Figure 5. ξ is almost unchanged with the reaction time in the first 100 min of irradiation and then steeply increases before approaching an intrinsic wavelength of ca. 3.7 μm. Since the cross-linking reaction proceeds inhomogeneously during irradiation, there is a strong possibility for the formation of local regions with quite different cross-linking densities in the reacted blend. Under this circumstance, local gradients of cross-linking densities might be produced in the samples and are magnified at longer irradiation times. Actually, the cross-linking kinetics data constructed from the changes in absorbance of anthracene for this (20/80) blend can be well expressed by the stretched exponential function.[12,14] This result supports the speculation that the kinetics of the inhomogenous cross-linking reactions is partially responsible for the spatial coherence emerging in Figure 4c.

(b) Nucleation-Assisted Spinodal Structures. These particular structures were formed by the nucleation and growth process followed by the spinodal decomposition under continuous irradiation. They appear when PSCS/PVME (50/50) and (70/30) blends are photo-cross-linked at 80 and 90 °C, respectively. Phase separation of a PSCS/PVME (50/50) blend becomes observable by phase-contrast optical microscopy at 30 min after irradiation at 80 °C. Compared to the blends with the same composition cross-linked at higher temperatures, phase separation took place at a longer irradiation time because the experimental temperature is located far away from the cloud point. Initially, small nuclei first appear at 30 min and become more obvious as the irradiation time increases. An example is shown in Figure 6a for a PSCS/PVME (50/50) blend obtained after 120 min of irradiation. Then the interconnecting structures appear around these nuclei and become

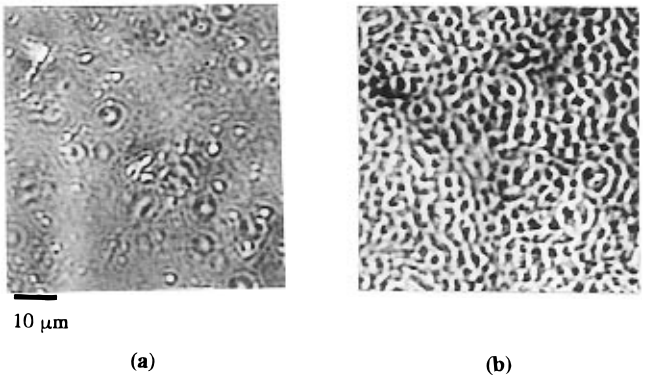

Figure 6. Phase-contrast optical micrographs of a PSCS/PVME (50/50) blend irradiated at 80 °C over (a) 120 min and (b) 480 min.

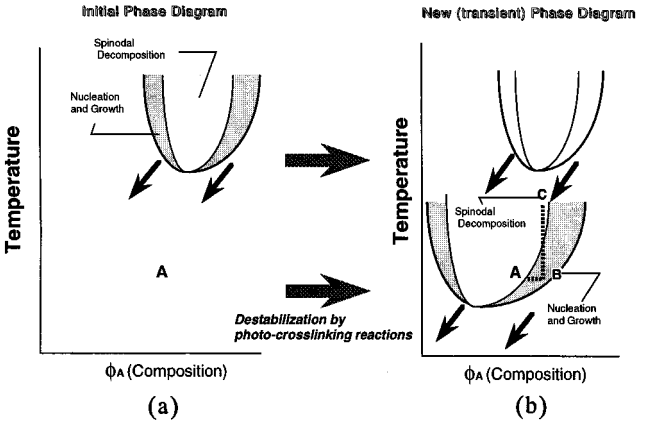

Figure 7. Proposed mechanism for the nucleation-assisted spinodal decomposition process.

remarkable as the irradiation time increases. These secondary structures grow with time until the phase separation process is frozen by the cross-linking reaction. The mechanism of this phase separation can be explained by the so-called nucleation-assisted spinodal decomposition process which is schematically illustrated in Figure 7. Namely, the PSCS component forms networks upon cross-linking, thermodynamically destabilizing the PSCS/PVME blend. Though the exact thermodynamical behavior such as phase equilibrium of cross-linked polymer blends is currently not well understood, their phase boundaries are expected to move toward the direction of smaller PSCS compositions, as indicated by the arrows in Figure 7a. Here, point A represents the experimental temperature of a blend with a given composition initially situated in the one-phase region. As the cross-linking density in the reacted blend reaches a critical threshold, the new coexistence curve crosses point A. For most cases, A will first enter the binodal region of the reacted blend, triggering the nucleation process at B, as illustrated in Figure 7b. Under this circumstance, if the phase boundary of the blend moves downward with an appropriate rate, it is possible for the nuclei formed at B to be stabilized. Under continuous irradiation, these stable nuclei will be brought into the unstable region of the blend via the path BC while the phase boundary is moving. Thus the spinodal decomposition process takes place, triggering the formation of the secondary morphology around point C. Generally, this process corresponds to jumping the blend *obliquely* along the temperature axis from the one-phase into the binodal region and successively into the spinodal region with a

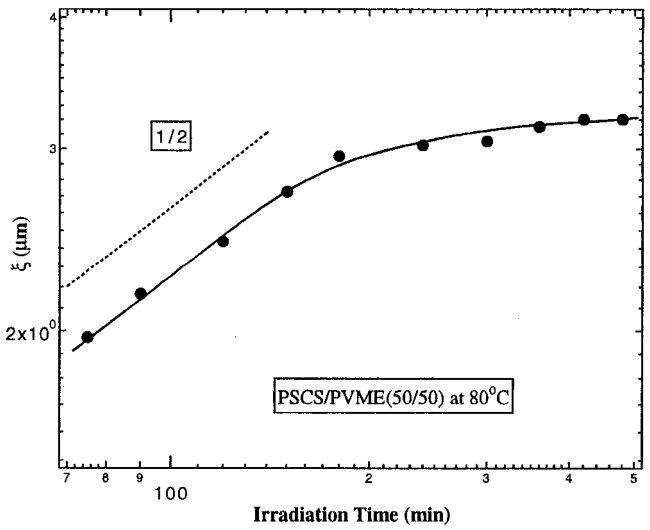

Figure 8. Irradiation time dependence of the average length scale ξ obtained for the interconnecting structures of a PSCS/PVME (50/50) blend cross-linked at 80 °C.

jump rate gradually deaccelerated by the cross-linking reactions. This *obliquity* comes from the modification of the blend composition by cross-linking. To analyze the phase separation kinetics of this particular case, ξ of the interconnecting structures emerging at a given irradiation time was measured by using a digital image analyzer. The characteristic length scale ξ which is the average value of the 10−15 data taken from the same morphology, is plotted versus irradiation time in Figure 8 under a double logarithmic scale. Similar to the case observed for the cross-linking reactions carried out at higher temperatures, ξ increases with irradiation time in the first 200 min and then tends to approach an equilibrium value of ca. 3.5 μm independent of irradiation time. As indicated in the figure, the growth of these cocontinuous structures in the early stage of the reaction follows the power law with the exponent $\alpha \cong 1/2$ which has been predicted for the phase separation kinetics in nonconserved systems.[15] In the nucleation-assisted spinodal decomposition process described above, this nonconservation of the order parameter probably comes from the competitions between the spinodal decomposition and the nucleation processes in the unstable region of the reacted blends.

(c) Concentric (Target) Patterns. As PSCS/PVME blends were photo-cross-linked at higher temperatures, concentric patterns appeared. These peculiar structures were obtained in the temperature range 90−110 °C and 100−110 °C for PSCS/PVME (50/50) and (70/30) blends, respectively. As reported previously, these target patterns become observable at ca. 60 min of irradiation. As irradiation time increases, their contrast becomes stronger whereas their sizes do not remarkably change.

Upon irradiation over a long time, the layers of these targets become disconnected and decompose into very regular spherical domains which are responsible for the higher-order diffraction patterns obtained by 2-dimensional light scattering.[14] Similar to the other cases obtained in this work, these structures were eventually frozen by the cross-linking reaction. Figure 9 shows the micrographs of the cross-section of a PSCS/PVME blend cross-linked at 90 °C over 600 min. The broken lamellae with the thickness comparable to the width of the target layers are obviously seen in this optical micrograph. Furthermore, the direction of these lamellae is almost perpendicular to the sample surface, suggesting that the target patterns observed in this work are not spherically but rather cylindrically symmetric with the axis parallel to the direction of irradiation. One of the reasons responsible for this result is that the UV light propagates through the sample from above to below. As observed in Figure 9, the phase-separated structures in the portion close to the bottom of the irradiated blend are somewhat unclear compared to those close to the top surface, implying that the region in the vicinity of the bottom is not significantly affected by irradiation. In other words, the photochemical reaction is not an efficient tool to control the morphology of thick samples. Nevertheless, for the case of anthracene, the gradient of light in the sample is not large because the absorption spectra of the photodimers are well separated from those of anthracene monomers, and particularly they almost do not overlap with the wavelengths of the exciting light. Therefore, experiments using PSCS/PVME blends thicker than 50 μm were not performed in this work. On the other hand, there exists a number of studies on the wetting effects on the phase behavior of polymer blends. These phenomena become remarkable when the sample thickness is smaller than a certain critical value which varies with the specific interactions between the substrate and the blend components. It has been reported that for polystyrene/poly(vinyl methyl ether) blends with glass used as a substrate, the threshold of the thickness for these wetting effects to take place is less than 10 μm[16] whereas it is ca. 20 μm for poly(vinyl acetate)/poly(methyl methacrylate) mixtures.[17] Therefore, to minimize the formation of the graded structures created by the gradient of light intensity in thick samples, and also to avoid the wetting effects arising from the substrate/polymer interactions in thin samples, 50 μm is probably the appropriate thickness for our experimental conditions.

(d) Possible Mechanism for the Target Pattern Formation. In order to explain the mechanism for the formation of the target patterns, Furukawa has recently studied the spinodal decomposition of binary mixtures in the presence of impurities such as nuclei by two-dimensional computer simulation.[18] It was found in these works that when the concentration of impurities (nuclei) is low so that the average distances between these nuclei are much larger than the intrinsic Cahn−Hilliard wavelengths of the system, the target patterns appear. However, when the density of the nuclei in the mixture is higher than a certain threshold, the target patterns disappear due to the interference of the spinodal waves propagating from these nuclei. The morphology obtained by computer simulation in the latter case resembles the nucleation-assisted-spinodal structures shown in Figure 6b. Experimentally, the number of layers around the nuclei is less than those seen in the computer simulation. This is probably due to the increase in viscosity of the blend with reaction time and, as a consequence, the spinodal waves cannot proceed far away from the nuclei as predicted by computer simulation. On the other hand, the mechanism for the formation of concentric patterns shown in Figure 9 for a PSCS/PVME (50/50) blend photo-cross-linked at 90 °C is currently not clearly understood though a series of experiments was carried out in an attempt to justify that these peculiar patterns are the fingerprints of interference phenomena.[19] The first possibility is that these patterns are the replica of the Newton rings generated by small gaps or ridges formed between the sample and the cover glass during the cross-linking

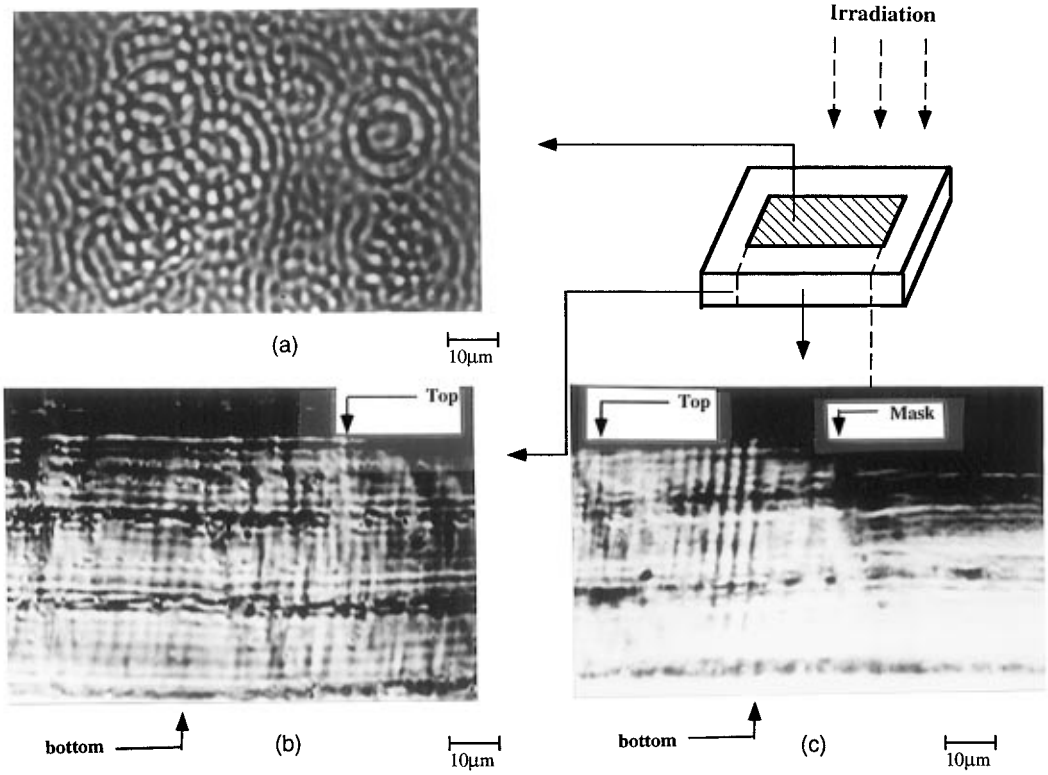

Figure 9. Target patterns obtained with a PSCS/PVME (50/50) blend photo-cross-linked over 10 h at 90 °C: (a) through view; (b) edge view at the middle part of the cross-section; (c) edge view at the border between the mask (right) and the blend film (left). The phase-separated (left) and the miscible (right) regions of the irradiated blends can be clearly seen in the figure.

Table 1. Modulated Phases Emerging from Photo-Cross-Linked Polymer Mixtures (Experimental conditions: Hg−Xe lamp, 3.0 mJ/(cm²·s))

region	morphology	evolution kinetics	mechanism
I (close to T_c[a])	interconnecting structures	following the scaling law $\xi(t) \propto t^{\alpha}G(t)$ with $\xi = 1/3 - 1/5$[10]	phase separation takes place inside the unstable region of the reacting blend and is eventually frozen
II (close to T_g[b])	metastably miscible semi-IPNs or microphase separation	phase-separated domains are limited in the nanometer scale	photo-cross-linking reaction overcomes the phase separation
III (less P(S-*stat*-CMS) fraction)	labyrinthine patterns, isotropy → anisotropy transition	the reacted blend passes through the Cahn−Hilliard region before approaching an intrinsic length scale	shallow quench with remarkable contribution of the elastic stress produced by the network formation
IV (nucleation-assisted spinodal decomposition)	coexistence of nuclei and interconnecting structures	the growth of the interconnecting structures follows the above scaling law with $\alpha = 1/2$	spinodal decomposition competes with nucleation in the unstable region
V (target-pattern formation)	concentric phase-separated structures	unchanged with time at the early stage and exhibiting period doubling-like behavior at later time	these structures might be initiated by the complex couplings between the cross-linking reaction and some optical effects associated with phase separation

[a] Cloud point. [b] Glass transition temperature.

process. However this explanation is not convincing because the light source used in these experiments is an incoherent Xe−Hg lamp with a broad wavelength distribution ranging from 300 to 700 nm. This property of the light source does not facilitate the interference phenomena. Furthermore, the squares of the target radii depicted in Figure 9 do not vary as an integer with the ring index, therefore disagreeing with the consequence of interference due to the Newton rings. Moreover, the imprinted interference patterns were not observed in the same blend when monodisperse polystyrene beads of 3 μm in diameter were placed on top of the blend during irradiation under the same conditions. From these results, it can be concluded that the interference, even possible, is not the only cause of these concentric patterns in photo-cross-linked blends. More elaborate experiments such as triggering the spinodal decomposition process of PSCS/PVME blends incorporated with cross-linked polymer beads might provide some convincing answers for the mechanism of the target pattern formation.

(3) Morphological Phase Diagram of Polymer Blends Photo-Cross-Linked in the One-Phase Region. From the experimental results described above, the morphological phase diagram was constructed and illustrated in Figure 10. Depending upon the competitions between the reactions and the phase separation kinetics, five distinct regions have been found for PSCS/PVME blends cross-linked in the miscible region located between the coexistence curve and the glass transition temperatures. These findings are summarized in Table 1. It is worth noting that this phase diagram can be

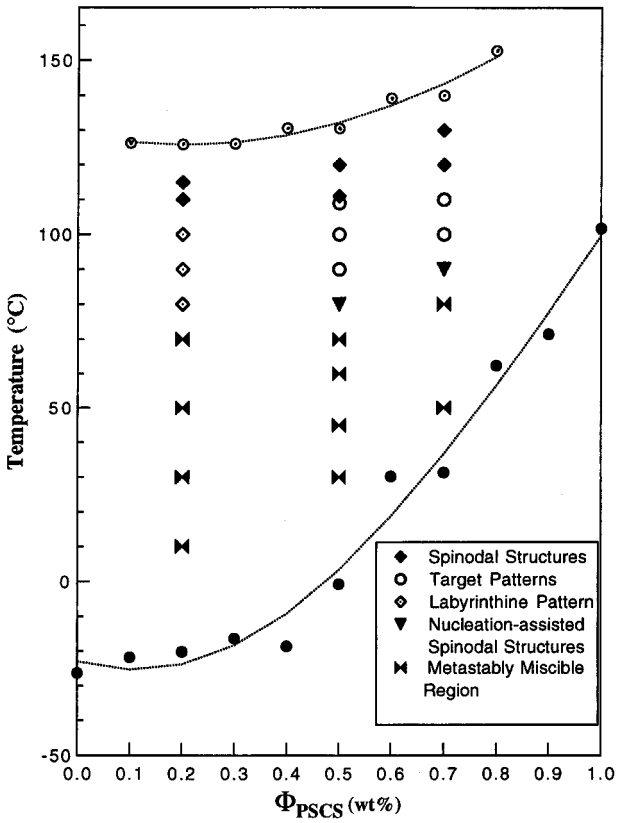

Figure 10. Morphological phase diagram of a PSCS/PVME blend photo-cross-linked in the one-phase region. Light source: 500 W Xe−Hg lamp. Light intensity at 365 nm: 3.0 mJ/(cm^2·s). (⊙) and (●) are the cloud points and the glass transition temperatures of PSCS/PVME blends before irradiation.

greatly modified by changing the reaction kinetics and therefore strongly depends on the external control parameters such as light intensity and the concentration of photo-cross-linkers. These phase diagrams might be useful for the morphological design of multiphase polymer materials. Recently, complicated phase diagrams were constructed for simultaneous interpenetrating polymer networks of polyurethane and poly(methyl methacrylate) based on the competition between phase separation and gelation.[20] Comparison of these results with the phase diagram illustrated in Figure 10 might give some insight into the significance of morphology control by thermally activated and photochemical reactions.

IV. Conclusion and Summary

It has been shown that a wide variety of ordered structures can be created and controlled by performing photo-cross-linking reactions of one component in a binary polymer mixture.

(1) From the technical points of view, the competition between phase separation and the cross-linking reaction can be efficiently controlled by photo-cross-linking reactions because, in comparison to thermally activated curing reactions such as those utilized in epoxy resins or other thermosetting polymers, the reaction can be quickly induced by light even at ambient temperature. On the other hand, photochemical reactions utilized for these purposes have two drawbacks. At first, the applicability of the techniques is limited by the sample thickness. Furthermore, irradiation becomes less efficient as the sample becomes cloudy. However, as demonstrated in this work, by using thin samples and a photo-cross-linker with neglible absorption at the exciting wavelength after reacting, photochemical reactions can provide a great tool to adjust the balance of phase separation and the cross-linking reactions for the morphology control.

(2) From the physical points of view, phase separation induced by chemical reactions is an interesting phase transition phenomena because the resulting morphology depends strongly on the competitions between antagonistic effects which can be controlled externally.[21,22] Furthermore, in principle, the symmetry of the free energy of the mixture with respect to the order parameter (composition) can be broken by changing the reaction orders. This aspect could lead to novel ordering phenomena in phase separation of reacting polymer blends. Particularly, for photo-cross-linking reactions, the elastic stress arising from the network formation becomes remarkable at the late stage of the reaction and can actively participate as a long-range effect on the phase separation process.[23,24] These important roles of elasticity can be elucidated by repeating the experiments with *non*-cross-linking photochemical reactions to induce phase separation of these PSCS/PVME blends. These works are currently in progress and will be reported later.

(3) Finally, from the viewpoint of mathematical modeling for these reaction-induced phase separations, it is, in general, necessary to take into account the effects of thermodynamics on the reaction kinetics.[25,26] Recently, a positive feedback loop driven by concentration fluctuations has been experimentally found for PSCS/PVME blends photo-cross-linked in the one-phase region under deep quench conditions.[12] These results suggest that it is necessary to incorporate the contribution of the concentration fluctuations induced by the cross-links into the reaction kinetics in order to model the ordering phenomena shown in this work.

In summary, phase separation of cross-linked polymer mixtures is a very complicated and interesting problem cutting across many scientific disciplines. The results shown in this work provide a basis for a novel morphological architecturing of multiphase polymeric materials by combining phase separation with chemical reactions.

Acknowledgment. The financial support from the Ministry of Education, Science, and Culture via a Grant-in-Aid on the Priority-Area-Research "Photoreaction Dynamics" No. 07228236 and a Grant-in-Aid for Scientific Research (C) No. 08651078 is gratefully acknowledged. We greatly benefited from the discussions with Takao Ohta (Department of Physics, Ochanomizu University, Japan) and Jack F. Douglas and Barry J. Bauer (Polymers Division, National Institute of Standards and Technology, Gaithersburg, MD).

References and Notes

(1) For example, see: Cross, M. C.; Hohenberg, P. C. *Rev. Mod. Phys.* **1993**, *65*, 851.

(2) For example, see: (a) Lee, J. L. Reaction Injection Molding. In *Comprehensive Polymer Science*; Allen, G., Bevington, J. C., Eds.; Pergamon Press: Oxford, 1989; Vol. 7; pp 379−426. (b) Brown, S. B.; Orlando, C. M. Reactive Extrusion. In *Encyclopedia of Polymer Science and Engineering*; John Wiley & Sons: New York, 1988; Vol. 14, pp 169−189.

(3) For example, see: *Polymeric Materials for Microelectronic Applications*: *Science and Technology*; Itoh, H., Tagawa, S., Horie, K., Eds.; Advances in Chemistry Series No. 579; American Chememical Society: Washington, DC, 1995.

(4) *Interpenetrating Polymer Networks*; Klempner, D., Sperling, L. H., Utracki, L. A., Eds; Advances in Chemistry Series No. 239; American Chemical Society: Washington, DC, 1994.
(5) For a review, see: Seul, M.; Andelman, D. *Science.***1995**, *267*, 476. For a computer simulation, see: Sagui, C.; Desai, R. C. *Phys. Rev. E* **1994**, *49*, 2225.
(6) Zasadzinski, J.; Schneider, M. B. *J. Phys.* (*Fr.*) **1987**, *48*, 2001.
(7) Bodenschatz, E.; de Bruyn, J. R.; Ahlers, G.; Cannel, D. S. *Phys. Rev. Lett.* **1991**, *67*, 3078.
(8) Tamai, T.; Imagawa, A.; Tran-Cong, Q. *Macromolecules* **1994**, *27*, 7486.
(9) Imagawa, A.; Tran-Cong, Q. *Macromolecules* **1995**, *28*, 8388.
(10) Harada, A.; Tran-Cong, Q. *Macromolecules* **1996**, *29*, 4801.
(11) Glotzer, S. C. Computer Simulation of Spinodal Decomposition in Polymer Blends. In *Annual Reviews of Computational Physics*; Stauffer, D., Ed.; World Scientific: Singapore, 1995: Vol. II, pp 1−46.
(12) Kataoka, K.; Harada, A.; Urakawa, O.; Tran-Cong, Q. To be published.
(13) Cahn, J. W.; Hilliard, J. E. *J. Chem. Phys.* **1958**, *28*, 258; **1959**, *31*, 688. Cahn, J. W. *Acta Metall.* **1961**, *9*, 795. Cahn, J. W. *J. Chem. Phys.* **1965**, *42*, 93.
(14) Tran-Cong, Q.; Harada, A. *Phys. Rev. Lett.* **1996**, *76*, 1162.
(15) Allen, M.; Cahn, J. W. *Acta Metall.* **1979**, *27*, 1085.
(16) Reich, S.; Cohen, Y. *J. Polym. Sci., Polym. Phys. Ed.* **1981**, *19*, 1255.
(17) Nesterov, A.; Horichko, V.; Lipatov, Y. *Makromol. Chem. Rapid Commun.* **1991**, *12*, 571.
(18) Furukawa, H. *J. Phys. Soc. Jpn.* **1994**, *63*, 3744, 3919.
(19) Harada, A.; Tran-Cong, Q. *Bussei Kenkyu* **1994**, *63*, 581.
(20) Mishra, V.; Du Prez, F. E.; Gosen, E.; Goethals, E. J.; Sperling, L. H. *J. Appl. Polym. Sci.* **1995**, *58*, 331.
(21) Glotzer, S. C.; Coniglio, A. *Phys. Rev. E* **1994**, *50*, 4241.
(22) Verdesca, J.; Borckmans, P.; Dewel, G. *Phys. Rev. E* **1995**, *52*, 4616.
(23) Nakazawa, H.; Sekimoto, K. *J. Chem. Phys.* **1996**, *104*, 1675.
(24) Cullis, A. G. *Mater. Res. Soc. Bull.* **1996**, *21*, 21 and other articles in this issue.
(25) Tran-Cong, Q.; Meisyo, K.; Ishida, Y.; Yano, O.; Soen, T.; Shibayama, M. *Macromolecules* **1992**, *25*, 2330. Tran-Cong, Q.; Ishida, Y.; Tanaka, A.; Soen, T. *Polym. Bull.* **1992**, *29*, 89.
(26) Lefever, R.; Carati, D.; Hassani, N. *Phys. Rev. Lett.* **1995**, *75*, 1674. Carati, D.; Lefever, R. Reprint.

MA961542X